

Impedance in the EMVCo Test Environment

Measurement and Calculation

White Paper by M. Gebhart
 Email: contact@rfid-systems.at

Abstract—Contactless Payment incorporates the Proximity Card specification for the physical-layer of the air interface. The physics is based on the coupling of resonant loop antenna circuits in the inductive near-field. Two main effects determine the near-field communication channel in the 13.56 MHz ISM frequency band: A strong decrease of H -field with increasing distance between reader and card, and a shift of resonance, or in fact a change of impedance. Understanding this impact on the reader antenna impedance as a function of coupling with the card, which also incorporates a certain impedance, is key to understanding all specified aspects of the physical-layer at the air interface. We investigate this impedance for the EMVCo test environment under operating conditions, with direct measurement and using analytical equations. We provide equivalent circuit element values for the specified test devices and also impedance values for positions in the operating volume.

Keywords—EMVCo, Contactless Payment, Inductive Coupling, Contactless Communication.

I. INTRODUCTION AND MOTIVATION

Contactless communication over a few centimeters between a reader and a battery-less card involves power transfer and bi-directional data transmission. The most prominent application today may be contactless payment, which uses this physical connection for encrypted data exchange. To assure interoperability between devices of different manufacturers, properties of this physical-layer are specified at the air interface, where the loop antennas of the reader and the card provide a contactless connection. Several aspects of power transfer and communication are considered, intensively characterized in the product development phase, and certified by authorized test laboratories before a product can be released.

The air interface is provided by conductor loops. It may be questioned whether these may be called antennas according to the modern definition, intending the emission of electromagnetic waves (in the far field), or just be called coupling inductors. Literature and standards in this field use the term antenna, and in fact these components will also emit electromagnetic waves although this is not the primary intention, much rather the application is limited to the near-field. The author likes to point out this *application difference* to conventional wireless communication by using the term *contactless* communication, and in accordance to literature and convention in this field, we will speak about loop antennas in this paper.

Coupling between the loop antennas, which are operated in resonance, is the effect which mainly determines the channel characteristics in the inductive near-field. The

influence of the card antenna circuit on the reader antenna circuit has a major impact on all properties specified at the physical layer. In fact, it changes the H -field which is continuously emitted by the reader at the 13.56 MHz carrier frequency. The H -field is used for contactless power transfer, so it is probably the most essential aspect for the air interface. Like all aspects it is specified in a range, from H_{MIN} to H_{MAX} . Other parameters are typically characterized as a function of the alternating H -field.

The underlying physical effect is a change in impedance of the reader antenna, due to the coupling with the current-carrying card antenna. To explain the influence of the so-called "card loading" on all aspects of the physical-layer specification at the air interface it is key to understand this impedance change. So, obviously the value of the H -field is not sufficient for a specification, it is also essential, under which card loading condition it is measured. This involves the test environment, specified in test specifications.

The specification for proximity card systems [1] was taken over by the Europay, MasterCard, Visa Contactless Consortium (EMVCo) for the specification of contactless payment [3]. However, the EMVCo test environment and method [3] is different from the ISO/IEC approach [2]. Like in the real application, it takes into account a variation of coupling between the proximity coupling device (EMVCo PCD [4]), which is emulating a payment terminal reader for testing real contactless credit cards, and the reference proximity integrated circuit card (EMVCo Ref PICC [5]), which is emulating a contactless card for testing real payment terminal readers. According to the EMVCo test concept indicated in fig. 1, the card is tested at specified positions of a specified operating volume (OV) over the terminal reader, as shown in fig. 2.

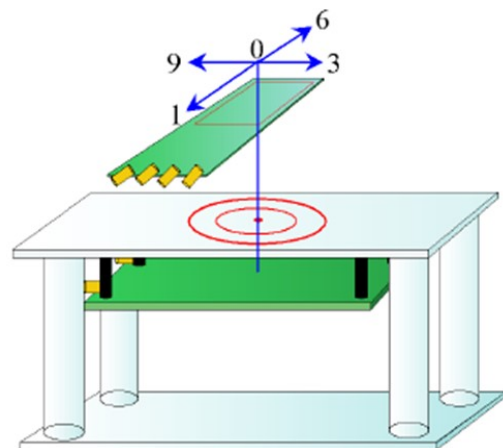


Fig. 1. Appearance and concept of EMVCo contactless testing.

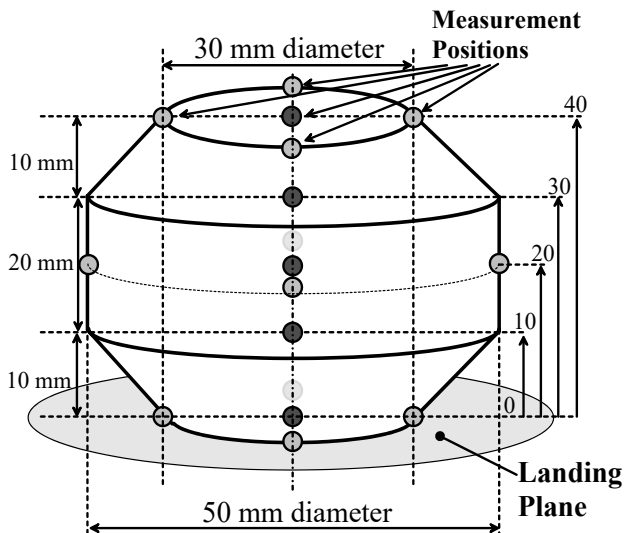


Fig. 2. EMVCo operating volume.

The EMVCo PCD alone, consisting of loop antenna and a simple matching network, has an impedance of $(50 + j0)$ Ohms at 13.56 MHz at the network input, where the lab amplifier is connected. In operating conditions the impedance deviates from this value due to coupling with a contactless card and depending on the position of the card in the operating volume.

The reference devices emulate real cards and readers. It can be insightful to investigate this impedance change caused by “card loading” for the example of the EMVCo specified test environment. In this paper, two methods are used to obtain the EMVCo PCD network input impedance at 13.56 MHz under coupling conditions: A measurement method at high operating RF power conditions using a specific set-up, discussed in section II, and a calculation method using equivalent circuit element and coupling factor values as input, discussed in section III. In section IV we compare results for both methods. This validates the calculation method, and our assumptions for the equivalent circuit representation of the EMVCo test environment.

II. FIRST OPTION: MEASUREMENT OF PCD IMPEDANCE UNDER OPERATING CONDITIONS

A straightforward approach is a direct measurement of the EMVCo PCD input impedance at 13.56 MHz in coupling to the EMVCo Ref PICC at each position in the operating volume. The main advantage of a direct measurement (compared to calculation) is that every effect which has an impact on the resulting impedance will be taken into account and no theoretical pre-assumptions are needed. E.g. metal plates or electronic circuitry, which may be part of a real device with NFC interface in card emulation mode, or parasitics in the circuit layout are accounted by direct impedance measurement.

The main difficulty is obtaining measurements at high power levels – in the range of several Watts – while also accurately measuring an impedance that deviates from the standard 50 Ohms.

The impedance is of interest at operating conditions, which are specified in the range between H_{MIN} and H_{MAX} . These conditions are specified to be measured with the Ref PICC for EMVCo. For a certain adjustment of the Ref PICC, basically a resonance frequency at 16.1 MHz for the antenna circuit, and a non-linear transistor shunt loading following an input rectifier, a specified DC voltage measure on the Ref PICC output is required. Depending on the position in the operating volume, limit values for this DC voltage are specified for the H_{MIN} and H_{MAX} condition. To be able to measure the appropriate impedance (which depends on the H -field strength) it is necessary to feed the EMVCo PCD with such high RF power at 13.56 MHz, so that DC voltages in the interesting range can be measured on the EMVCo Ref PICC at each position in the OV. Table I gives the specification for the DC voltage depending on the position, and measured PCD feed impedance.

Impedance at RF frequencies is usually either measured with an impedance analyzer (bridge instrument) or with a network analyzer (using a directive coupler). According to our research, there is no instrument commercially available, which would support the requirement of at least 1 W RF power at 13.56 MHz measurement frequency. Network and impedance analyzers all operate at lower power levels, e.g. up to 10 dBm into a 50 Ohm termination, which corresponds to 10 mW. So it seems necessary to build a measurement set-up consisting of an analyzer which allows to connect an external, high-power directive coupler, and to boost the RF source with an external amplifier to the required power level. We have developed such a set-up and published it in [7], where we had used it for a specific chip characterization. The concept is indicated in fig. 3. It has proven to be a useful tool also for the characterization of passive components like inductors for NFC operating conditions, and the set-up can also be used for direct impedance measurement for the EMVCo PCD to Ref PICC coupling in the operating volume for the range of operating power conditions. Fig. 4 – 9 show our results in linear plots and Smith charts.

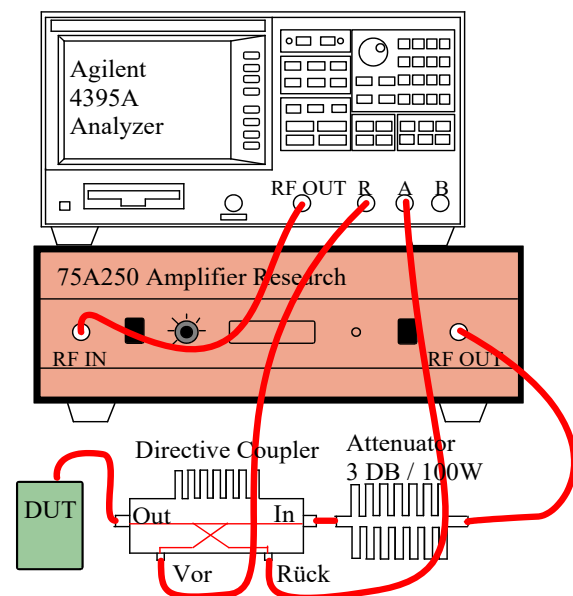


Fig. 3. High RF power impedance measurement set-up.

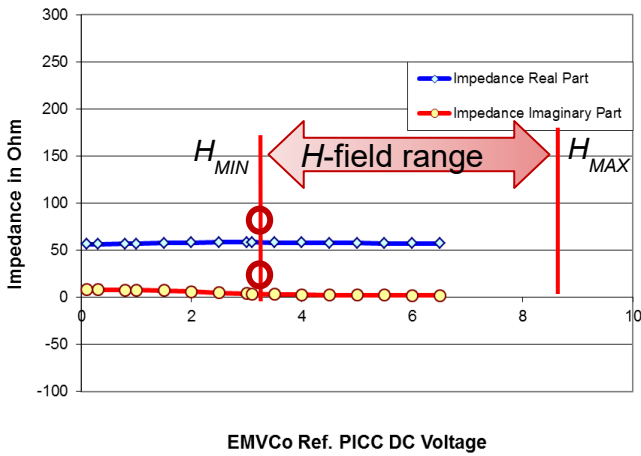


Fig. 4. Impedance in real and imaginary part as function of DC voltage.

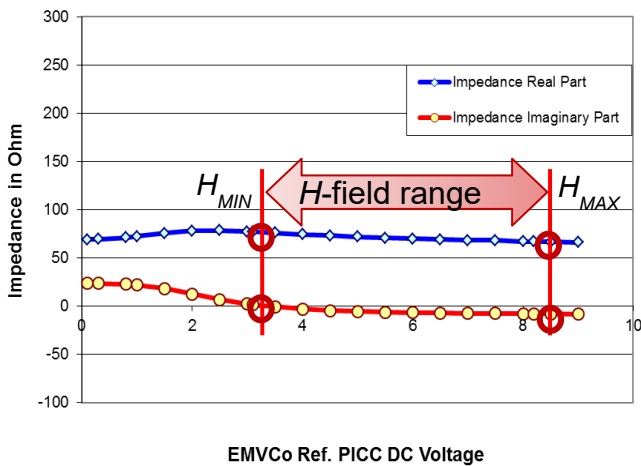


Fig. 5. Impedance in real and imaginary part as function of DC voltage.

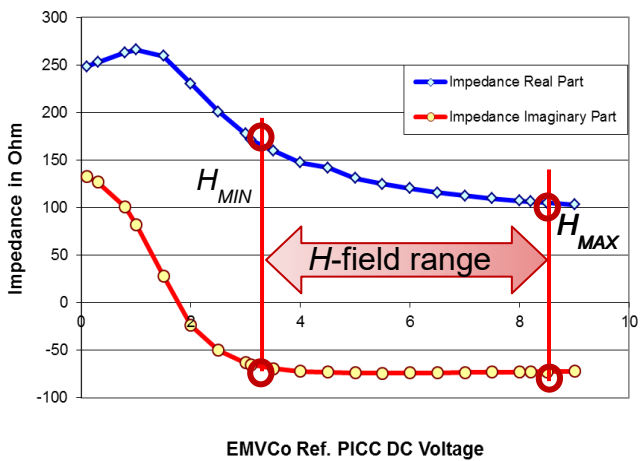


Fig. 6. EMVCo PCD feed impedance in real and imaginary part as function of EMVCo Ref PICC DC voltage measured at J9.

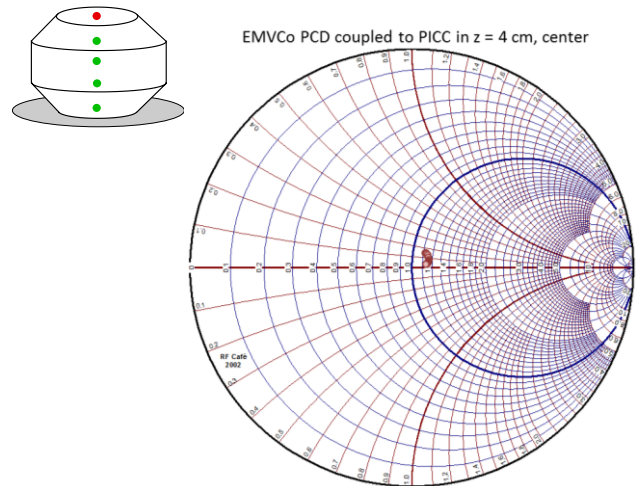


Fig. 7. Impedance at PCD network input over H -field range in $z = 4$ cm.

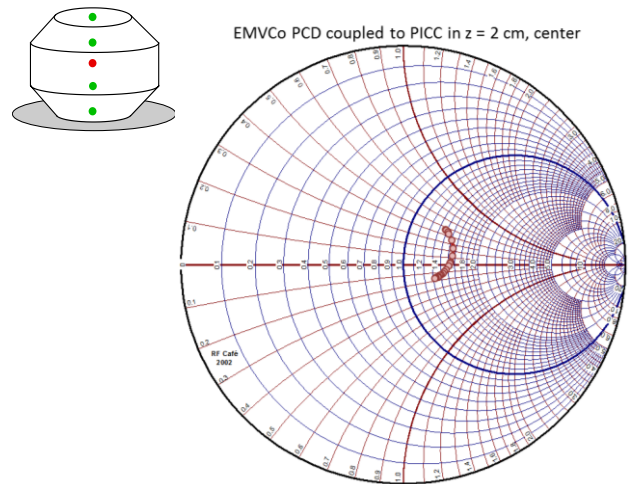


Fig. 8. Impedance at PCD network input over H -field range in $z = 2$ cm.

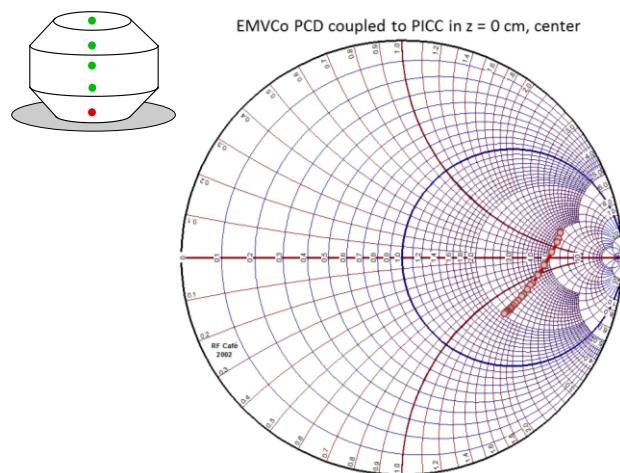


Fig. 9. Measured impedance at PCD network input over H -field range (covering the H_{MIN} and H_{MAX} points) in $z = 0$ cm distance over landing plane.

TABLE I. SPECIFIED EMVCo REF PICC CONDITION AND MEASURED PCD IMPEDANCE

EMVCo PCD to Ref PICC coupling						
OV	H_{MIN} condition			H_{MAX} condition		
Dist.	Ref PICC	Re(Z)	Im(Z)	Ref PICC	Re(Z)	Im(Z)
cm	V(DC)	Ω	Ω	V(DC)	Ω	Ω
0	3.10	171.0	-65.5	8.2	106.2	-72.9
1	3.05	108.4	-8.3	8.2	81.6	-25.7
2	3.00	77.3	2.1	8.2	66.8	-8.1
3	2.78	63.8	3.6	8.2	59.7	-1.0
4	2.55	58.3	4.7	8.2	n.A.	n.A.

III. SECOND OPTION: CALCULATION OF PCD IMPEDANCE UNDER OPERATING CONDITIONS

A. Overview

Alternatively (only for air coils) we can also calculate the impedance of the EMVCo PCD in coupling to the EMVCo PICC. Our calculation method uses an analytic formula approach and gives the impedance at the carrier frequency under operating RF power and near-field coupling conditions. As an input it requires

- an equivalent circuit representation for the Ref PICC under operating RF power conditions,
- the coupling between PCD and PICC loop antenna for each position of interest in the operating volume,
- an equivalent circuit representation for the PCD loop antenna,
- and the PCD matching network towards the RF power feed point.

The equivalent circuit structure is the typical simplified representation of a loop antenna [8], consisting of inductance in series to resistance, parallel to capacitance. The element values can either be measured, according to a procedure also given in [9], or may be calculated from the antenna layout using a finite-element simulation software (FEM), or can be estimated using analytical formulas [10]. The antenna resonant circuits of both, PCD and Ref PICC are power-independent, as we have verified for the interesting RF power range. For the EMVCo PCD, also the matching network is power-independent. This is not the case for the network of the EMVCo Ref PICC, which must be set to the “non-linear load” condition for reader H -field measurement. As a DC voltage output of the Ref PICC defines the H_{MIN} and H_{MAX} conditions in the EMVCo specification, we need to find the corresponding antenna RF voltage amplitudes and the equivalent linear impedances for these operating conditions.

EMVCo PCD coupled to PICC in z var., center

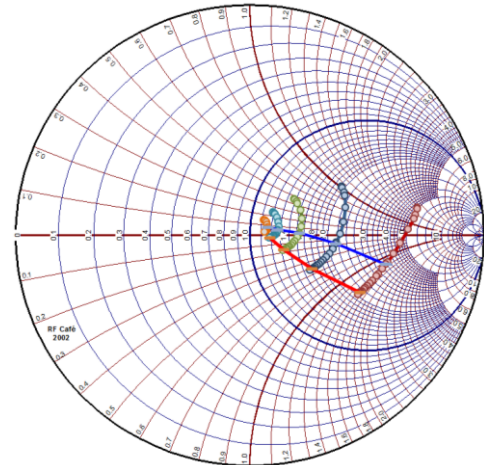


Fig. 10. EMVCo PCD input impedance at 13.56 MHz with H_{MIN} , H_{MAX} limits for Ref PICC at 5 distances in center positions of the operating volume.

For the coupling of the Ref PICC loop antenna to the PCD loop antenna we derive analytical formulas based on an equivalent T-structure circuit representing the inductive coupling.

Table II and table III give a summary of all required data to calculate the impedance at carrier frequency under operating conditions. The following sub-sections $B - E$ explain, how these values were obtained. In sub-section F we introduce a model to calculate the PCD impedance under Ref PICC card loading.

TABLE II. EQUIVALENT CIRCUIT ELEMENT, MATCHING NETWORK AND COUPLING FACTOR VALUES

EMVCo PCD and PICC loop antenna equivalent circuit					
Element	Value	Unit	Element	Value	Unit
L_{PCD}	0.62	μH	L_{PICC}	2.29	μH
R_{PCD}	2.1	Ω	R_{PICC}	0.8	Ω
C_{PCD}	35.2	pF	C_{PICC}	41.7	pF
EMVCo PCD matching network components, and transformation					
Element	Value	Unit	Ratio	Value	Unit
C_P	141.8	pF	T	0.5203	---
C_S	46.9	pF			
Coupling and mutual inductance in distance					
Distance	k	Unit	M	Unit	
0 cm	0.210	---	2.24	μH	
2 cm	0.082	---	0.088	μH	
3 cm	0.038	---	0.039	μH	

Technical White Paper

B. EMVCo Ref PICC equivalent circuit

The EMVCo Ref PICC consists of a loop antenna resonance circuit, connected to a diode bridge rectifier, to which different loads can be connected over switches [5]. For H -field measurement it is specified to connect a shunt load built of several transistor stages. The impedance of this circuit is power-dependent, it is also called “non-linear load” in the specification document [3]. The DC voltage measured in parallel to this non-linear load is the specified indication for H -field strength. So it is the parameter which is finally needed to characterize a contactless reader.

In a 1st step the antenna and variable capacitor for a Ref PICC, adjusted according to specification (resonance at 16.1 MHz for a specified measurement method), were disconnected from the remaining circuit and the equivalent circuit element values were measured. These L_{PICC} , R_{PICC} , C_{PICC} values are given in table II. Most important of these is the antenna inductance L_{PICC} , which is required for a later calculation step.

Impedance values for the non-linear load, or the complete Ref PICC, are more difficult to obtain. In principle the equivalent DC voltage and linearized impedance at one operating power condition could either be simulated e.g. in SPICE [14], or measured in the lab using the high-RF-power impedance measurement set-up which we have already introduced in section II. Diodes and transistors have significant voltage production tolerances and temperature dependency, leading to quite a significant spread of a simulated DC voltage. It is better to measure a look-up table between the antenna RF voltage amplitude, and the DC voltage output of a well-calibrated Ref PICC under room temperature conditions.

A SMA connector in parallel to the loop antenna is available on the Ref PICC. The complete Ref PICC (which is set to “non-linear load” mode) is used as a DUT (using J6 in [5]) and connected to our high-power impedance measurement bench [7]. Our measurement results are given in table III. H_{MIN} and H_{MAX} conditions are marked in bold and red text color.

TABLE III. EMVCo REF PICC PARAMETERS

EMVCo Ref PICC v. 2.1 Impedance Measurement					
ISO/IEC H -field			EMVCo Ref PICC		
$V(rms)$	$A/m(rms)$	$V(DC)$	$V(rms)$	$Re(Z)$ in Ω	$Im(Z)$ in Ω
0.19	0.59	0.1	1.534	355	751
0.32	0.99	1.0	2.751	525	688
0.44	1.38	2.0	4.377	700	358
0.63	1.98	3.1	5.700	559	149
0.82	2.55	4.0	6.656	477	75
1.14	3.57	5.5	8.115	398	24
1.49	4.65	7.0	9.609	349	0
1.78	5.56	8.2	10.682	325	-10.1
1.95	6.11	9.0	11.52	312	-16
2.62	8.19	12.0	14.26	282	-28

C. Coupling between PCD and PICC loop antenna

From all effects, as represented by Maxwells set of equations, we only take into account the magnetic coupling, as we are in the inductive near-field and this can be assumed to be the dominating effect. Magnetic coupling over the H -field can either be calculated, or measured, e.g. according to the widely used voltage-ratio method described in [12]. Both approaches are simplifications, so we have compared measurement results with the result of an analytical calculation, and found a good agreement. Results for the coupling factors in distances of 15 mm for the “landing plane” of the operating volume above the EMVCo PCD loop antenna, plus distances of all center positions in the OV (this means 0, 1, 2, 3 and 4 cm above the landing plane) are again provided in table II. As it can be rarely found in literature, we provide the analytical formula which we have used.

Mutual inductance can be calculated by solving the Neumann integral formulas [13]. For two planar rectangular loop antennas in cartesian coordinates (positioned in the xy -plane with distance z) with average conductor length a and conductor width b , this results the analytical equation (1) for the geometry part m_{GEO} of the mutual inductance.

$$\begin{aligned}
 m_{GEO} = & \int_{-\frac{a_1}{2}}^{\frac{a_1}{2}} \int_{-\frac{a_2}{2}}^{\frac{a_2}{2}} \frac{1}{\sqrt{h_r^2 + \left(\frac{b_2}{2} + z_0 - \frac{b_1}{2}\right)^2 + (y_2 + y_0 - y_1)^2}} dy_2 dy_1 + \\
 & + \int_{-\frac{a_1}{2}}^{\frac{a_1}{2}} \int_{-\frac{a_2}{2}}^{\frac{a_2}{2}} \frac{-1}{\sqrt{h_r^2 + \left(\frac{-b_2}{2} + z_0 - \frac{b_1}{2}\right)^2 + (y_2 + y_0 - y_1)^2}} dy_2 dy_1 + \\
 & + \int_{-\frac{a_1}{2}}^{\frac{a_1}{2}} \int_{-\frac{a_2}{2}}^{\frac{a_2}{2}} \frac{-1}{\sqrt{h_r^2 + \left(\frac{b_2}{2} + z_0 + \frac{b_1}{2}\right)^2 + (y_2 + y_0 - y_1)^2}} dy_2 dy_1 + \\
 & + \int_{-\frac{a_1}{2}}^{\frac{a_1}{2}} \int_{-\frac{a_2}{2}}^{\frac{a_2}{2}} \frac{1}{\sqrt{h_r^2 + \left(\frac{-b_2}{2} + z_0 + \frac{b_1}{2}\right)^2 + (y_2 + y_0 - y_1)^2}} dy_2 dy_1 + \\
 & + \int_{-\frac{b_1}{2}}^{\frac{b_1}{2}} \int_{-\frac{b_2}{2}}^{\frac{b_2}{2}} \frac{1}{\sqrt{h_r^2 + \left(\frac{a_2}{2} + y_0 - \frac{a_1}{2}\right)^2 + (z_2 + z_0 - z_1)^2}} dz_2 dz_1 + \\
 & + \int_{-\frac{b_1}{2}}^{\frac{b_1}{2}} \int_{-\frac{b_2}{2}}^{\frac{b_2}{2}} \frac{-1}{\sqrt{h_r^2 + \left(\frac{-a_2}{2} + y_0 - \frac{a_1}{2}\right)^2 + (z_2 + z_0 - z_1)^2}} dz_2 dz_1 + \\
 & + \int_{-\frac{b_1}{2}}^{\frac{b_1}{2}} \int_{-\frac{b_2}{2}}^{\frac{b_2}{2}} \frac{-1}{\sqrt{h_r^2 + \left(\frac{a_2}{2} + y_0 + \frac{a_1}{2}\right)^2 + (z_2 + z_0 - z_1)^2}} dz_2 dz_1 + \\
 & + \int_{-\frac{b_1}{2}}^{\frac{b_1}{2}} \int_{-\frac{b_2}{2}}^{\frac{b_2}{2}} \frac{1}{\sqrt{h_r^2 + \left(\frac{-a_2}{2} + y_0 + \frac{a_1}{2}\right)^2 + (z_2 + z_0 - z_1)^2}} dz_2 dz_1
 \end{aligned} \tag{1}$$

Index 1 means the first loop antenna (in our case the PCD), index 2 means the second loop antenna (in our case the PICC). x_0, y_0 and z_0 mean a center of the 1st loop antenna which is different from the origin.

Two rectangular loop antennas are the most typical case, although in the EMVCo test environment the PCD has a circular loop antenna. So we have used a square of equal area, to calculate a_1 and the equal b_1 .

The mutual inductance M can then be calculated according to (2)

$$M = \frac{\mu_0}{4\pi} N_1 N_2 \cdot \cos(\alpha) \cdot m_{GEO} \quad (2)$$

where μ_0 is the permeability constant, N_1 is the number of conductor turns of the 1st loop antenna, N_2 is the number of conductor turns of the 2nd loop, α is an optional slant angle (in our case, as both antennas are in the xy-plane, set to 0) and m_{GEO} is the above mentioned geometrical part of mutual inductance.

The magnetic coupling factor k between EMVCo PCD and Ref PICC can then be calculated from the inductance of both antennas and the mutual inductance, according to (3)

$$k = \frac{M}{\sqrt{L_1 \cdot L_2}} \quad (3)$$

D. EMVCo PCD equivalent circuit

The PCD consists of a (electrically compensated) loop antenna resonance circuit with external resistor to lower the Q-factor, connected to an L-structure type matching network consisting of serial and parallel capacitor [4].

We have dis-connected the antenna layout from the matching network by cutting a connection on the board layout. Then we could measure the PCD loop antenna equivalent circuit elements in a similar manner as the Ref PICC. Values are again provided in table II.

E. PCD matching network

To obtain values of the serial and parallel capacitor in the matching network, we have disconnected and measured these components using a precision LCR Meter at 13.56 MHz. However, there may be small measurement errors, and additional layout parasitics are difficult to measure. So our approach was to calculate the theoretical values for the two capacitors in order to properly adjust the antenna impedance to 50 Ohms at the network input or RF power feed point. The calculation was done according to the method given in [11]. Then we did compare with measured capacitor values, to judge if everything fits within measurement tolerances. The values we obtained in this way are again given in table II. As the matching network magnifies any error in the antenna equivalent circuit or in the network, precision is important here. Furthermore, we recommend as a first step in the final impedance calculation, to verify the 50 Ohm input impedance of the PCD with no coupling. This is also displayed with a cross-mark in figures 12 – 14.

F. Equivalent T-structure model for magnetic coupling

At this point, we have all the required input data to calculate the PCD feed impedance under card loading conditions. If we neglect other effects and focus on coupling over the magnetic flux, we can model the air interface between the two antenna inductances with an idealized transformer, as shown in fig. 11. Without coupling, the primary (PCD) side shall have an inductance L_1 , and the secondary (PICC) side shall have an inductance L_2 . If the primary inductance is current-carrying, an H -field will be emitted. As per this model, due to coupling a part of this magnetic flux will penetrate the second inductance L_2 . We can imagine a part of L_1 which we call M , is emitting the part of the flux, which penetrates L_2 . This M will be totally coupled (at $k = 1$) to a part of L_2 , which we also call M . Since M is equal on primary and secondary side, we can combine the two equations, as the voltage across M will be equal. This is the idea of the equivalent T-structure model for magnetic coupling, which is also shown in fig. 11. In the general case, we also need to take into account the transformation ratio T , which equals the turn ratio of primary (N_1) and secondary (N_2) coil, or the square-root of the inductance ratio

$$T = \frac{N_1}{N_2} = \sqrt{\frac{L_1}{L_2}} \quad (4)$$

The second side, and the load impedance of the secondary inductance are also affected by this transformation. Using this model approach, we can now calculate the PCD loop antenna impedance under card loading conditions.

In section IIB, tab. III, we have measured the complete Ref PICC impedance $Z_M = R_M + jX_M$, in parallel to the antenna. To apply the T-structure model, we need Z_{TL} , so we have to exclude the loop antenna inductance L_{PICC} . This is given in (5)

$$Z_{TL} = \left(R_{PICC} + \frac{1}{\frac{1}{Z_M} - \frac{1}{R_{PICC} + j\omega L_{PICC}}} \right), \quad (5)$$

where R_{PICC} is the Ref PICC antenna resistance. Values for L_{PICC} and R_{PICC} are given in tab. II.

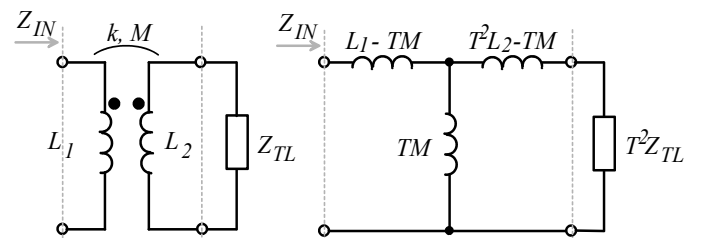


Fig. 11. Transformer model for magnetic coupling and equivalent T-structure.

In our next step, the impedance for the inductance of the primary antenna, $j\omega L_{PCD}$, is replaced by the impedance of our equivalent T-structure model, Z_{IN} . This is calculated according to

$$Z_{IN} = j\omega(L_{A1} - TM) + \frac{1}{\frac{1}{T^2 Z_{TL}} + j\omega(T^2 L_{A2} - TM)} + \frac{1}{j\omega TM} \quad (6)$$

For the impedance of the complete PCD antenna, we need to take into account the other elements of the simple equivalent circuit which we had extracted in section IID.

$$Z_{PCD} = \frac{R_{A1} + j\omega L_{A1}}{1 + j\omega R_{A1} C_{A1} + j\omega L_{A1} \cdot j\omega C_{A1}}$$

$\xrightarrow{\text{CARD LOADING}}$

$$= \frac{R_{A1} + Z_{IN}}{1 + j\omega R_{A1} C_{A1} + Z_{IN} \cdot j\omega C_{A1}} \quad (7)$$

Finally, we have to transform the new EMVCo PCD antenna, using the parallel and serial capacitors of the simple matching network, to obtain the feed impedance Z_F at the PCD RF input connector. This is given by

$$Z_F = \frac{1}{\frac{1}{Z_{PCD}} + j\omega C_P} - j\frac{1}{\omega C_S} \quad (8)$$

The results of this calculation are provided in figures 12 – 14. They give the calculated EMVCo PCD feed impedance in the Smith chart in blue circles for a range of operating power points for the (linearized) EMVCo Ref PICC impedance, as given in tab. III. We have again selected the same 3 points in the operating volume for distances of 0, 2, and 3 cm to the landing plane, resulting in coupling factors given in tab. II.

For comparison we have also taken over the directly measured impedances and show them in red circle points. To note: The impedance of the PCD without card loading was adjusted to $(50 + j0)$ Ohms (before measurement, and before calculation of the loaded impedance). This is marked with a cross.

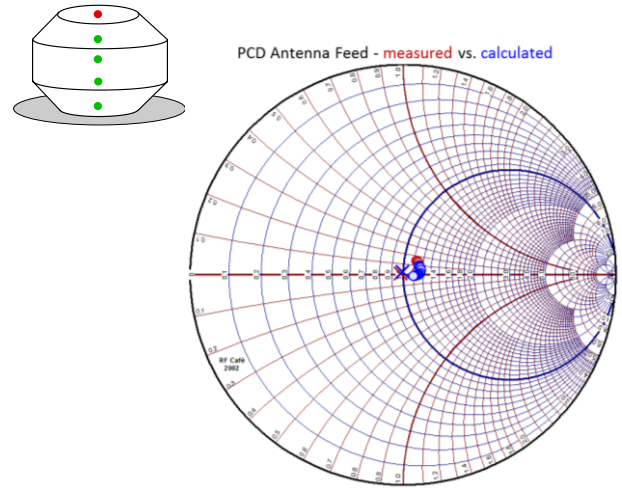


Fig. 12. Impedance at PCD network input over H -field range in $z = 4$ cm.

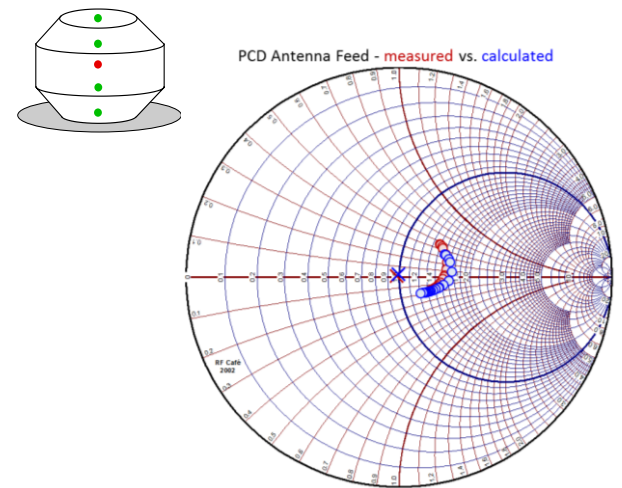


Fig. 13. Impedance at PCD network input over H -field range in $z = 2$ cm

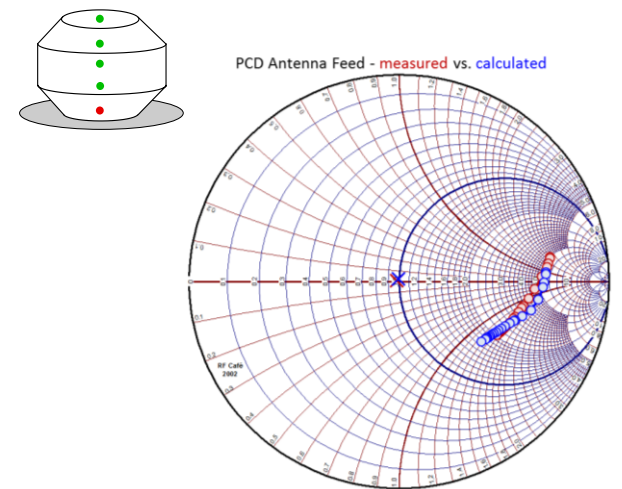


Fig. 14. Calculated & measured impedance at PCD network input over H -field range (covering the H_{MIN} and H_{MAX} points) in $z = 0$ cm

IV. SUMMARY AND CONCLUSION

We have presented two methods to obtain the impedance of a contactless reader antenna network under card loading conditions, a lab measurement method and an analytic calculation model. We have selected the EMVCo test environment to apply our methods. These are well-specified components which are also of a high practical use, as they are relevant for certification of products for contactless payment.

Impedance values obtained for coupling at different distances in center positions of the operating volume and between H_{MIN} and H_{MAX} operating RF power conditions, given in tab 1 and fig. 10, show quite a significant deviation of up to 350 % from 50 Ohms as the nominal value for typical lab equipment. It can also be seen that the H_{MIN} condition provides the stronger loading impact. This can be explained by a higher PICC antenna current due to a higher Q -factor in the parallel loop antenna resonance circuit. Overall, fig. 10 proofs valid the initial statement, the H -field amplitude is also depending on measurement conditions. For the specified operating range (H -field), the impedance varies significantly.

The comparison between direct measurement and the presented analytical calculation method shows similar results. Alternative calculation methods can be found in literature, e.g. in [10], but care should be taken: Some methods may depend on preconditions and thus may not be applicable on a general problem as treated here, or contain simplifications. Also for our results, there is not a perfect fit. This may have several reasons:

In general, direct measurement would be the preferred method in practice, especially as it is able to take into account the impact of metal parts or other circuits which have influence. A problem is the high required measurement power at 13.56 MHz, which cannot be generated by any commercially available analyzer instrument. The calculation method can be applied on air coils, if no other parts nearby take influence on the impedance. This approach can even be used, if no lab prototype is available for measurements. However, as the method depends on several input parameters, it is more complex and sensitive to deviations of the input data, especially on the PCD equivalent circuit element values. It is also based on several approximations and simplifications. E.g. electrical coupling, besides the dominating magnetic coupling, may have a non-negligible effect for very small distances.

Furthermore, it may be easy to calculate with coupling factors, but their exact value is in fact difficult to obtain – by measurement and calculation. However, the matching of results between the two methods seems sufficient for building up RF system estimations. Such estimations are very useful in this field.

For an engineer working in conventional *wireless* communication, this may give an idea of the main aspects of work in *contactless* communication. And all this was considered just for a single frequency, the 13.56 MHz carrier alternating H -field, which is responsible for contactless power transfer from reader to card. Reader modulation, and sensitivity to card load modulation require to consider a frequency range, which introduces one more dimension in complexity.

REFERENCES

- [1] ISO/IEC 14443:2011(E), *Identification cards – Contactless integrated circuit cards – Proximity cards – Part 1, 2, 3 and 4*, ISO, Geneva, Switzerland, 2008 - 2011.
- [2] ISO/IEC10373-6: *Identification cards – Test methods – Part 6: Proximity Cards*. ISO, Geneva, Switzerland, 2011.
- [3] EMV® Contactless Specifications for Payment Systems, *Book D – EMV Contactless Communication Protocol Specification, V. 2.1*. EMVCo, LLC, March 2011.
- [4] MasterCard International Inc., *PayPass Reference Equipment – Reference PCD Manual*, Version 1.5, May 2007.
- [5] MasterCard International Inc., *PayPass Reference Equipment – Reference PICC Manual*, Version 1.3, May 2007.
- [6] MasterCard International Inc., *PayPass Reference Equipment – Reference CMR Manual*, Version 0.1 + DR, May 2007.
- [7] M. Gebhart, J. Bruckbauer, M. Gossar, „Chip Impedance Characterization for Contactless Proximity Personal Cards”, 7th CNSDSP, pp. 826 – 830, July 2010, Newcastle, UK.
- [8] M. Gebhart, M. Wobak, E. Merlin, C. Chlestil, “Active load modulation for contactless near-field communication”, 3rd RFID-TA, pp. 228 – 233, Nov. 2012, Nice.
- [9] M. Gebhart, R. Neubauer, M. Stark, D. Warnez, „Design of 13,56 MHz Smartcard stickers with ferrite for payment and authentication”, 3rd Workshop on NFC, pp. 59 – 64, ISBN 978-0-7695-4327-7, Feb. 2011, Hagenberg, Austria.
- [10] K. Finkenzyler, *RFID-Handbuch: Grundlagen und praktische Anwendungen von Transpondern, kontaktlosen Chipkarten und NFC*, 6. Edition Carl Hanser Verlag GmbH & Co. KG, Mai 2012.
- [11] M. Gebhart, T. Baier, M. Faccini, “Automated Antenna Impedance adjustment for NFC”, 12th ConTEL, pp. 235 – 242, June 2013, Zagreb.
- [12] S. Hackl, C. Lanschützer, P. Raggam, W. L. Randeu, „A novel method for determining the mutual inductance for 13.56 MHz RFID Systems”, 6th CNSDSP, pp. 297 –300, July 2008, Graz.
- [13] F. E. Neumann, “Allgemeine Gesetze der inducirten elektrischen Ströme”, *Abhandlungen der Königlichen Akademie der Wissenschaften zu Berlin*, Seiten 1 – 87, 1845.
- [14] Linear Technology, *LTspice IV Simulation Software*, (www.linear.com/designtools/software/), 2012 (online; accessed March 13th, 2012).
- [15] Peter Scholtz, *Analysis and numerical modeling of inductively coupled antenna systems*, PhD thesis at TU Darmstadt (<http://tuprints.ulb.tu-darmstadt.de>), Oct. 2010.
- [16] G. Manzi, “EMV Contactless Payment Systems based on AS3911”, CST European User Conference, May 2012, Mannheim, BRD.
- [17] U. Muehlmann, M. Gebhart, M. Wobak, "Mutual Coupling Modeling of NFC Antennas by Using Open-Source CAD/FEM Tools", 3rd Conf. on RFID TA, Nov. 2012, Nice, France.
- [18] <http://www.rfid-systems.at>